Available online at www.sciencedirect.com
SCIENCE DIRECT®
ELSEVIER
International Journal of Solids and Structures 42 (2005) 4519–4540
INTERNATIONAL JOURNAL OF SOLIDS and STRUCTURES
www.elsevier.com/locate/ijsolstr

Wavy-edged fractures in axially split aluminium tubes

Z. Zou, S.R. Reid *

Department of Mechanical, Aerospace and Manufacturing Engineering, University of Manchester, UMIST, Sackville Street, Manchester M60 1QD, UK

Received 21 January 2005
Available online 4 March 2005

Abstract

This paper is motivated by the somewhat unusual need to gain insight into the phenomenology of the mechanism by which a wavy edge is formed on the wreckage of some aircraft fuselage skins associated with aircraft destroyed in flight by on-board explosion.

In order to explore the role of the plastic zone adjacent to the crack tip whilst avoiding the practical complications of generating the fractures explosively, simple quasi-static experiments have been carried out on aluminium tubes. Oversized rigid dies were pushed inside the tubes along their axes to generate fractures in Mode I and Mode III. It is conjectured that wavy edges are associated with fractures resulting from internal expansion of the tube by a travelling, internal, radial ring pressure region. The pressurised region behind the crack tip would be produced by explosively generated internal pressure being vented at the crack and, for the purpose of this study, is considered to be equivalent to that generated by the die. The production of such cracks is clearly demonstrated experimentally and contrasted with the plain-edge fractures produces during Mode III tearing fracture.

A damage-model-based finite element analysis has been conducted to simulate the propagation of the crack and provide further insight into the strain and stress fields along the fractured edges. Both the experimental and numerical results show that this particular type of ring loading has to be applied to the tube to produce the wavy edge. Such a load expands the fractured flaps in the radial direction, stretching the material in the circumferential direction and, crucially, in the axial direction. The latter generates a relatively wide plastic wake close to and parallel to the fracture edge as the tube fails within which axial plastic strain predominates. Constrained by the remaining part of the tube that has not undergone plastic deformation, sufficient axial residual compressive stress can be produced in the plastic wake to produce a wavy edge which results from local buckling in the plastic wake. This mechanism suggests that ripples observed on the edges of fuselage skin wreckage are possible signatures of an internal explosion. The work described

* Corresponding author. Tel.: +44 161 300 3848; fax: +44 161 300 3849.
E-mail address: steve.reid@manchester.ac.uk (S.R. Reid).

0020-7683/$ - see front matter
doi:10.1016/j.ijsolstr.2005.01.016

herein is also relevant to the deformation in a failed high-pressure gas pipe following the propagation of a ductile crack as noted previously in the literature.

Keywords: Fracture; Local buckling; Plastic deformation; Tube; Wavy edge

1. Introduction

A motivation for the study described herein is that ripples in regions adjacent to the edges with amplitudes perpendicular to the plane of the panel, seen as wavy edges, have been observed occasionally on portions of the fuselage skin recovered from the wreckage of aeroplanes destroyed by internal explosions. It is obvious that a crack or tear has been initiated first in the skin, possibly due to internal overload, and has then propagated a long distance. The objective of this study is to demonstrate that such edges are Mode I fractures resulting from a moving internal pressure source rather than Mode III fractures that could be the consequence of, say, portions of the fuselage being torn away by aerodynamic forces.

This wavy edge bears strong similarities to the geometry of the edges of fractures produced in ductile cracks in high-pressure pipelines (Abbassian and Calladine, 1989) and in a study of split tubes (Reddy and Reid, 1986). An explanation for the waviness can be deduced from the contents of Abbassian and Calladine (1989). It can be ascribed to the development of a plastic wake left behind the propagating crack front. The wavy edge is in fact a local buckling phenomenon caused by the residual compressive stress in the direction parallel to the fracture edge. As such it is distinctive and appears to result from the propagation of a Mode I fracture that is driven primarily by an in-plane tensile stress field. As will be shown, the effect contrasts strongly with the result of a Mode III tear in which the forces driving the crack act out of the plane. The study below suggests strongly that recovered pieces of skin with this characteristic out-of-plane waviness were separated from the fuselage as the result of internal over-pressurisation. This would generate the necessary high circumferential stresses in the skin and so the presence of such a fracture morphology could be a useful forensic tool in analysing aircraft failures. However, the contrast between the edges of fractures produced under predominantly Mode I and Mode III conditions is itself instructive and will form the substantive part of this paper.

It is well known that, because of the high stress concentration at the tip of a crack, there is generally a plastic zone around the crack tip in a ductile metal structure. However, under general loading conditions, this plastic zone is very small and the largest plastic strain component is usually perpendicular to the crack. Preliminary experiments, performed on edge cracked flat aluminium thin plates under uniform in-plane tensile loading perpendicular to the crack as part of the present investigation, indicated that the plastic deformation was confined to a narrow band along the crack and no ripple was generated. Numerical simulations also showed that the magnitude of the plastic strain parallel to the crack is very low under these loading conditions and, to the author's best knowledge, no wavy-edge crack phenomena have been reported for such plates in the literature.

The deformation of circular metal tubes axially compressed onto a tapered circular die was examined experimentally by Reddy and Reid (1986). It was found that the tube normally split following the formation of a number of axial cracks and that the strips so formed were bent into curls. However, when the strips between the cracks were prevented from curling by use of a constraining plate, ripples were observed on the flattened strips of annealed aluminium tubes. Abbassian and Calladine (1989) investigated the deformation of a pipe wall during propagation of a ductile crack in a high-pressure gas pipeline. Plastic axial stretching was considered to be the prime mode of deformation of the pipe wall adjacent to the crack

(plastic wake zone). It was noted that the pipe adopts a generally U-shaped form with a characteristic rippled, wavy edge beyond the flap region downstream of the crack tip.

Apart from the aforementioned work, no systematic study of the conditions under which these wavy edges are formed has been reported. It turns out to be an interesting and challenging problem to address both experimentally and computationally. The aim of this study was to examine and possibly confirm the contention that the wavy-edge phenomenon is related to a Mode I loading condition as opposed to Mode III loading. The former would stem from high hoop stresses generated by high internal pressure. The latter could result from external agencies (such as wind loads) ripping away partially separated segments of the fuselage in the aeroplane example. There is evidence of the latter in other recovered parts of the fuselage. However the presence of this particular form of Mode I failure with the wavy characteristics described herein would appear to be strong evidence of failure due to internal over-pressurisation and is consistent with the effects of an internal explosion in the vicinity of the recovered section.

Extensive work can be found in the literature on gas-pressurised pipelines to determine the propagation and arrest characteristics of long-running ductile fractures (Ives et al., 1974; Shannon and Wells, 1974; Steverding and Nieberlein, 1974; Freund et al., 1976). Due to the escape of the gas, the pressure reduced rapidly in a small region behind the crack tip. It was found that the crack driving force is not derived from the internal pressure acting just ahead of the fracture. It appears instead that the crack is driven by the residual pressure acting on the flaps formed by the separated pipe walls behind the crack tip. The energy required to propagate a crack in a ductile pipe material is provided by the work done by the exhausting gas on the fracturing pipe.

It is evident that the ductile fracture propagation caused by the internal pressure in a pipeline is very complex. It involves a strong interaction between the dynamics of the escaping gas and the deformation of the pipe wall. The problem is highly nonlinear and a complete solution is not feasible. Simplification has to be made to capture the main features of interest.

In this paper, the results of experiments performed on thin-walled (diameter to thickness ratio, $D/t \approx 30$) aluminium tubes to investigate the wavy edge phenomenon are presented. Oversized rigid dies of different geometries were pushed into the tube to cause it to split and the resulting cracks to propagate axially. Essentially conical dies of short length, axially symmetric and non-symmetric, were used in the splitting tests. Efforts were made (e.g. by providing a starter-crack with a short fine cut in the end of the tube) to produce a single axial crack in the tube to form two flaps behind the crack tip. Another wedge die was designed to perform tube-tearing tests. It was observed that the conical dies expanded the tube significantly in the radial direction and several produced flaps with rippled edges. However, the wedge die caused little residual deformation of the edges of the flaps, in particular no ripple was produced.

To provide a more detailed insight into the wavy-edge phenomenon, numerical modelling was also performed to simulate both the conical and wedge die tests and to investigate the distribution and variation of the plastic strain in the tube. It was found that significant axial stretching occurs in the tube split by a conical die. For the wedge-tearing test, almost no axial stretching was found in the tube and the plastic zone was very small.

The conical die applies a similar ring pressure region to the tube behind the crack tip as does the escaping gas in a pressurised pipeline, or an internally explosive-expanded aircraft fuselage. It was postulated that radial expansion tests using a conical die of limited length could simulate the explosive fracture problem for the fuselage, whilst recognising that additional inertia forces and strain-rate dependency of the material properties would play additional roles. The coincidence of the wavy-edge fracture phenomenon with that of a radial outward 'travelling' load could be of great interest since it would strongly suggest that the wavy edge on the portion of the fuselage skin recovered from the wreckage of an aeroplane could have been caused by some kind of travelling radial transverse load acting on it. The contention is that initiating a Mode I fracture in the skin in this way, the internal pressure could drive the crack tip, leaving a stretched plastic wake behind it accompanied by wavy edges on the resulting flaps.

2. Experimental investigation

2.1. Specimens and test set-up

The tests performed were aimed at examining the generic difference between Mode I and Mode III fractures, not at simulating the aircraft or pipeline situation directly. Aluminium tubes of 50.8 mm outside diameter, 1.6 mm wall thickness were tested in their as-received and annealed conditions. Tubes were annealed by soaking at 360 °C for 30 min and allowed to cool in the furnace. Three types of die were used, axially symmetric and non-symmetric conical dies of limited length and a cylinder with a wedge attachment, for insertion into the tubes. The dies were attached to a steel rod, 320 mm long. They are shown in Fig. 1. The tube and the dies were lubricated. During the fracture test, the tube was placed on the rigid base of an Instron universal testing machine and the die was pushed into it at a speed of 20 mm/min to facilitate the logging of the force-die movement trace.

Tubes for the conical die tests were 300 mm long in order to reach a steady-state deformation condition. A single saw-cut was made at their upper ends. For the wedge die test, the tubes were 200 mm long and had two saw-cuts 30 mm apart at one end. The cuts provided starter cracks for the subsequent fracture of the tubes.

2.2. Conical die tests

An axially symmetric conical die was used first. The split tubes are shown in Fig. 2. The diameter of the cylindrical nose section (and the start of the tapered cone) was 46 mm and the cone angle was 12°. Both as-received and annealed tubes were tested. Only one crack initiated at the saw-cut. Crack propagation in the as-received tube is not in straight line but changed its direction twice. There seems to be a half-ripple on the flaps. It is not clear whether or not the ripple was caused by local buckling since it is located at the same position at which crack changed its direction. The annealed tube was split axially in straight line. As the crack length reached approximately 200 mm, a ripple appeared on the flaps. A die with a cone angle of 20° was also tested on an annealed tube. It generated multiple fractures. The tube split into several strips that scrolled and showed no ripples along the edges of the fractures. Similar behaviour was observed in the tube-splitting experiments of Reddy and Reid (1986). An explanation for the number of cracks formed in the steady state has been proposed by Atkins (1987) and will not be pursued here.

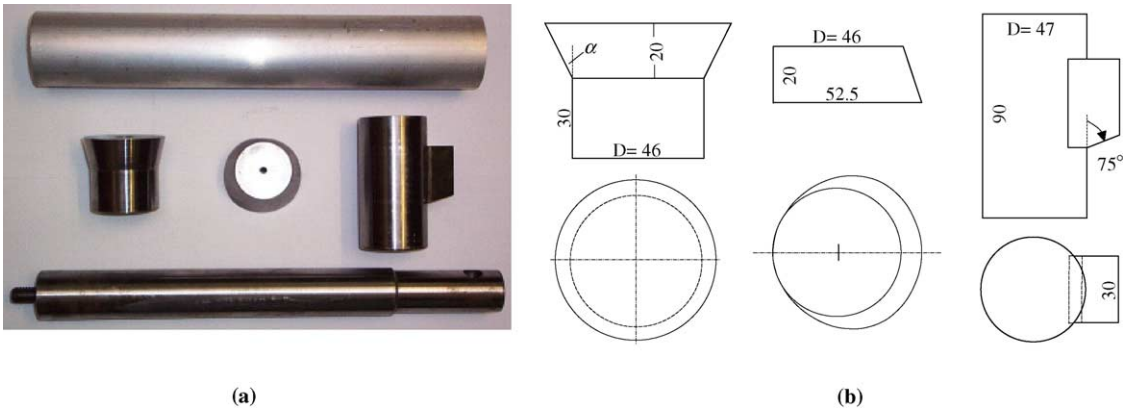

Fig. 1. (a) Tubes, dies and steel bar and (b) dimensions of the dies (in mm).

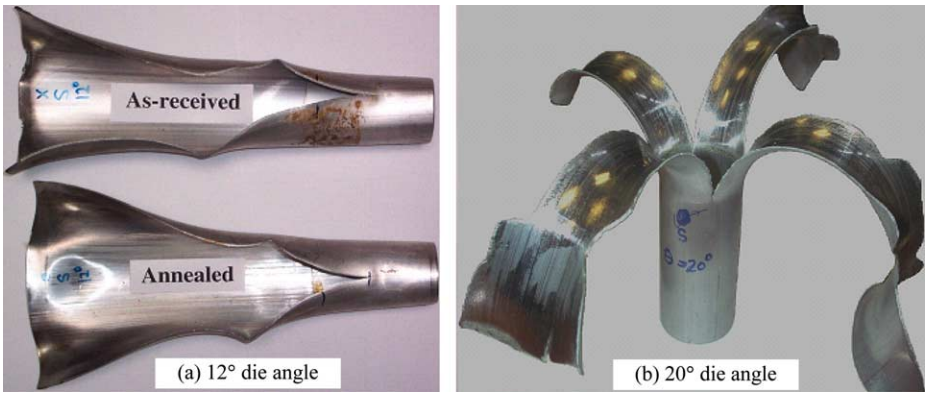

Fig. 2. (a) Tubes split with symmetrical 12° conical die. (b) Multiple splits with 20° die angle.

A non-symmetric (basically) conical die was then manufactured by reducing the cone angle over the greater part of an axially symmetric cone. The die had an axially symmetric nose section and axially non-symmetric base section. However, it still had a plane of symmetry that coincided with the saw cut during the test. The part with the maximum cone angle was placed to face the saw-cut. The non-symmetric conical die makes it much easier to grow the fractures only from the saw-cut and propagate them along the generator of the tube. Because the stretching and expansion of the tube are confined to the part around the crack, the cone angle could be made larger than in the symmetric one. Steady states were achieved earlier and more ripples were obtained. More importantly, the non-symmetric condition resembles more the localised explosive pressure distribution on a fuselage skin.

A die with a maximum cone angle of 18° produced wavy-edge fractures successfully and several annealed tubes were tested. The split specimens are shown in Fig. 3, most of them with two wavelengths of ripples on their fractured flaps. Single cracks were initiated at the saw cut and propagated in a straightforward manner along the generator. The crack tip remained very close to the nose of the cone die during the splitting process. After approximately 150 mm of crack propagation, a ripple gradually appeared on the flaps, much earlier than that in the symmetric cone tests. The ripples retained their size and position after their

Fig. 3. Tubes split with unsymmetrical conical die.

appearance and were 'laid down' as the crack propagated. It can be seen in Fig. 3, the two flaps could have different axial deformation pattern and hence on occasions showed ripples with different first peak positions and slightly different wavelength on the two flaps. Since the contention is that the wavy zones result from buckling of the edge regions that have residual axial plastic strain, variants are presumably due to some imperfection sensitivity in the buckling process. No parametric study was conducted since the focus was on the phenomenon, not its variants.

Fig. 4 shows the three typical deformation zones in a split tube. At the end of the tube the circular cross-section is almost flattened due to the opening up of the flaps. Away from the end, the tube cannot expand freely due to the constraint from the neighbouring uncracked parts and the deformation reaches a steady state, the edges of the two flaps becoming on average parallel to each other and to the axis of the tube. The constraint that terminates the divergence of the two edges of the flaps now imposes compressive stress on regions adjacent to the edges that have undergone stretching parallel to the edge leading to local buckling, seen as the wavy edges. Close to the crack tip, the tube wall has expanded radially and in the process zone close to the tip the material experiences the axial stretching which results in the wavy edge as described above. The cracked edges make an angle with the tube axis in the plan view. The larger the angle, the more severe are the expansion and stretching. The whole tube adopts a U-shaped form with the characteristic rippled, wavy edge behind the flap region as mentioned in Abbassian and Calladine (1989).

2.3. Wedge die tests

Because of the loading conditions, the tube splitting tests described above using conical dies result in a predominantly Mode I fractures. Mode III dominated tearing tests were also performed on the tubes. The die used comprised a wedge attached to a solid cylinder. The diameter of the cylinder was 47 mm, 0.6 mm less than the tube internal diameter. The wedge was 30 mm wide and its plane was at 75° to the tube axis. Initially two saw cuts were made on the edge of the tube separated by a distance equal to the width of the wedge.

Tested annealed and as-received tubes are shown in Fig. 5. A strip was torn from the annealed tube by the wedge. No expansion of the tube took place behind the fracture front. Apart for the coiled strip, the tube is essentially undeformed. No flaps are produced and there were no ripples on the strip edges. The curled strip on the tube is almost flat in the width (circumferential) direction, unlike the flaps observed in the conical die tests. The strip on the as-received tube cracked into three sub-strips which broke off sometimes as the strip curled up.

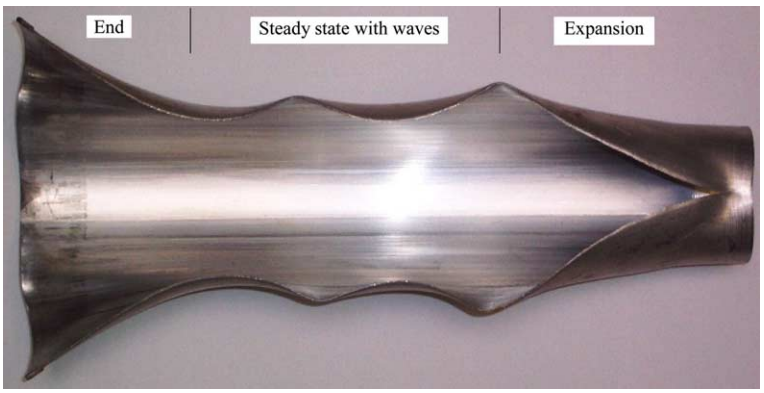

Fig. 4. Deformation zones on the 'buckled' wavy flaps.

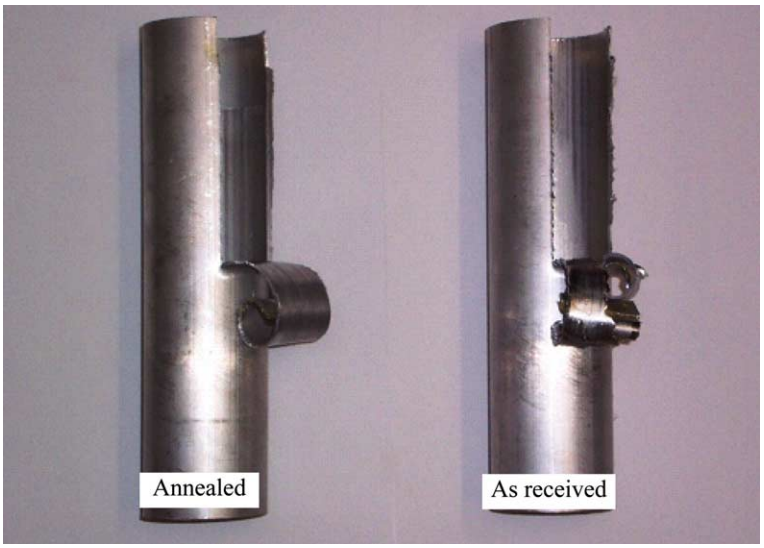

Fig. 5. Tubes torn with wedge die.

2.4. Brief summary of the test results

The tests performed demonstrated clearly the difference in fracture edge geometries that can be produced under Mode I and Mode III loading conditions. The wavy wake behind the Mode I fracture is affected by the plastic properties of the tubes, annealing producing a clearer demonstration of the phenomenon. No attempt was made in this study to examine extensively the influence of the tube or die geometry or the detailed influence of the material parameters. The tests were simply designed and performed to illustrate the prevalence of the wavy-edge fracture phenomenon for Mode I (internal pressure driven) cracks in cylindrical components.

3. Finite element analysis of the tests

To provide a more detailed understanding of the wavy edge phenomenon, numerical modelling of the two key problems was performed, simulating both conical and wedge die tests by using the commercial finite element code ABAQUS (HKS, 2001). Attention was mainly given to investigating the global deformation of the tubes and the distribution and variation of the strain and stress field in the tube for a chosen set of process parameters (geometry and material properties).

It was assumed that only one crack exists in the tube split by the conical die and two cracks in the wedge tearing tube and that the cracks propagate along their original direction. No new cracks were allowed to initiate and propagate elsewhere. Four-noded shell elements S4R were used to model an aluminium tube of mean radius 24.6 mm. The rigid die (cone or wedge) was modelled by rigid element R3D4. A contact pair, i.e. a slave surface containing all the nodes of the tube and the master rigid surface of the cone or wedge die, was defined to permit the contact between the tube and die to be simulated. Geometrical non-linearity was also included to assist in predicting the buckling, i.e. the formation of the ripple on the cracked flaps.

Plastic deformation has to be included in the analysis. The tests conducted on the annealed tubes were simulated. The measured uni-axial stress–strain behaviour for the annealed aluminium is given in Fig. 6,

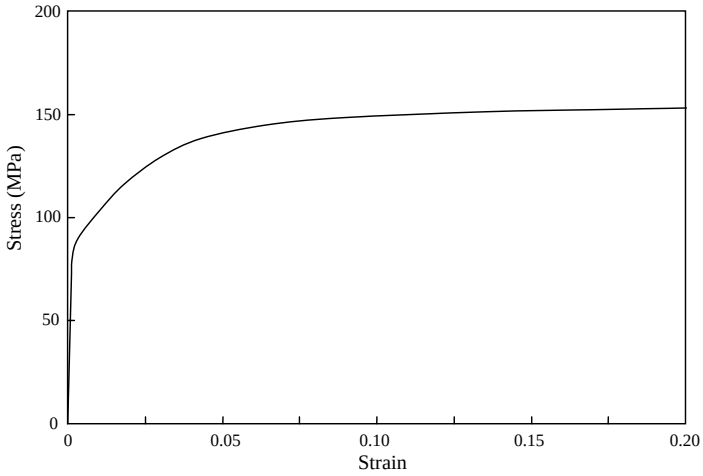

Fig. 6. Stress–strain curve for annealed aluminum.

with the Young's modulus $E = 70$ GPa and Poisson's ratio $v = 0.3$. The initial yield stress was taken as 85 MPa and the form and nature of strain hardening in the plastic region was taken to that shown in Fig. 6.

To model progressive crack propagation, an interface element was adopted and implemented into ABAQUS (HKS, 2001) via the user subroutine UEL (user element). Along the crack propagation line, duplicate nodes were introduced into the finite element mesh to generate two potential fracture edges. The interface element defines the characteristics of the connection between the two edges. If the crack propagates through an interface element, the connection breaks and two free surfaces (edges) are formed. The connection behaviour of the interface was governed by a continuum damage model proposed by the authors which has found successful application in delamination in composite laminates (Zou et al., 2003) and failure prediction of nuclear graphite (Zou et al., 2004). This model is described below briefly.

3.1. A continuum damage model for crack propagation

The major elements of this approach have been explained in detail in two recent publications by Zou et al. (2003, 2004). Consequently, below only the basic steps in the modelling are enumerated. For detailed explanations the readers are referred to these two publications. In this fracture model, an interface is introduced into the continuum solids at the position where potential crack surfaces may form, as shown in Fig. 7. The fracture process is modelled as a progressive damage mechanism at the interface. A damage surface is constructed which combines the conventional stress-based and fracture-mechanics-based failure criteria. The damage surface shrinks in the stress space as damage develops. As a result, a softening interfacial constitutive law is obtained, similar to the cohesive constitutive law employed in the literature (Needleman, 1987; Tvergaard and Hutchinson, 1992; Xu and Needleman, 1994). This model has its advantage over the cohesive model. The elements of the model are related back to the more usual engineering description of fracture/failure behaviour (material strength and critical energy release rates). Mode interaction is included naturally in the model if the failure criteria employed are interactive.

The interface has no thickness and perfect connection exists across the interface before damage initiation. As the load level increases, damage may initiate and fracture gradually develops at the interface. A

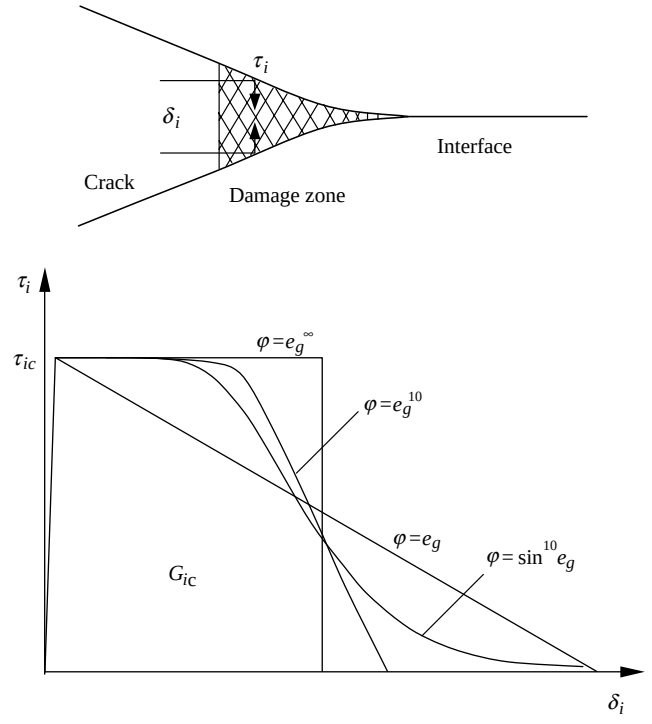

Fig. 7. Crack, damage zone, interface and interfacial traction–relative displacement curves.

damage parameter ω is introduced and the interfacial constitutive law is expressed as functions of the damage parameter to take account of the effects of damage as follows:

$$\tau_i = (1-\omega)k\delta_i \quad (i = 1,2,3), \tag{1}$$

where τ_i are the tractions on the interface and δ_i the relative displacement components across the interface. Subscript 1 indicates the through-thickness direction, and 2 and 3 are the other two orthogonal directions in the interface plane. k is a constraint or penalty stiffness of the interface within a range of 10^7–10^9 N mm^{-3}.

A damage surface is constructed as follows:

$$F(\tau_i, G_i) = e_s + \varphi(e_g) - 1 = 0, \tag{2}$$

where e_s is a stress-based failure criterion and e_g a fracture-mechanics-based criterion. φ is a monotonically increasing function of e_g satisfying $\varphi(0) = 0$ and $\varphi(1) = 1$. Energy dissipations G_i is defined as

$$G_i = \int \tau_i \mathrm{d}\delta_i \quad (i = \mathrm{I}, \mathrm{II}, \mathrm{III}). \tag{3}$$

In the present paper, e_s and e_g are chosen as follows

$$e_s = \frac{\tau_1^2}{\tau_{1c}^2} + \frac{\tau_2^2}{\tau_{2c}^2} + \frac{\tau_3^2}{\tau_{3c}^2} \quad \text{if } \tau_1 > 0 \tag{4}$$

or

$$e_s = \frac{\tau_2^2}{\tau_{2c}^2} + \frac{\tau_3^2}{\tau_{3c}^2} \quad \text{if } \tau_1 < 0 \tag{5}$$

and

$$e_g = \frac{G_I}{G_{Ic}} + \frac{G_{II}}{G_{IIc}} + \frac{G_{III}}{G_{IIIc}}, \tag{6}$$

where τ_{1c}, τ_{2c} and τ_{3c} are the interfacial tensile and shear strengths. G_{ic} ($i = I, II, III$) are the conventional individual critical energy release rates.

The damage surface is so constructed that a softening interfacial constitutive relationship is established. Before damage initiation, the initial stiffness of the interface is very large to simulate a perfect connection. As the relative displacement increases from zero, the traction increases rapidly. Once the stress based failure function e_s reaches unity, damage initiates. As relative displacement continues to increase, damage develops and e_g increases rapidly. This results in a shrinking damage surface in the stress space and consequently lower stresses are required for further damage as expected. When the fracture mechanics based failure function e_g equals unity, the traction is reduced to zero and complete cracked surfaces are formed.

When the damage surface is exceeded, i.e. the damage process begins,

$$F(\tau_i, G_i) = e_s + \varphi(e_g) - 1 > 0. \tag{7}$$

The incremental interfacial constitutive law and damage evolution law can be obtained in terms of incremental relative displacements as

$$d\tau_i = (1-\omega)k\,d\delta_i - k\delta_i \sum_{j=1}^{3} D_j d\delta_j, \tag{8}$$

$$d\omega = \sum_{i=1}^{3} D_i\,d\delta_i, \tag{9}$$

where

$$D_i = \left[\frac{\partial F}{\partial \tau_i}(1-\omega)k + \frac{\partial F}{\partial G_i}\tau_i\right] \Big/ \sum_{j=1}^{3} \frac{\partial F}{\partial \tau_j} k\delta_j. \tag{10}$$

When the interfacial stresses terminate within the damage surface, i.e.

$$F(\tau_i, G_i) = e_s + \varphi(e_g) - 1 < 0, \tag{11}$$

no damage development can occur, thus

$$d\omega = 0 \tag{12}$$

and the incremental constitutive law becomes

$$d\tau_i = (1-\omega)k\,d\delta_i. \tag{13}$$

This situation may happen in the case of low stress level or local unloading.

An interface element was developed to implement the above continuum damage model into the commercial finite element code ABAQUS (HKS, 2001) via the user subroutine UEL (user element). Dual coincident nodes along the likely crack path are required in the FE mesh. Each interface element has four nodes, two pairs of duplicated nodes, to connect two four-noded shell elements.

The material properties for the interface element were chosen as $G_{Ic} = G_{IIc} = G_{IIIc} = 50\ \text{kJ m}^{-2}$, $\tau_{1c} = 170$ MPa and $\tau_{2c} = \tau_{3c} = 98$ MPa.

Choosing different forms of φ for the damage surface produces different constitutive relationships for the interface as illustrated in Fig. 7. Assuming $\varphi = e_g$, a bilinear curve is produced for the single-mode case

which is often employed in the literature. When $\varphi = e_g^{10}$, a trapezoidal curve is achieved. An elastic perfect-plastic curve is obtained if $\varphi = e_g^{\infty}$. For the ductile aluminium material, it is preferable to employ the elastic perfect-plastic curve. However, the sudden release of the interfacial traction may cause severe solution convergence problems. Considering that the present problem involves four types of non-linearities: plasticity, contact, buckling and cracking, a smooth interfacial constitutive curve helps to improve the solution convergence rate. Therefore trapezoidal-like curve was generated by choosing $\varphi = \sin^{10} e_g$. This constitutive curve maintains the main features of the elastic perfect-plastic curve. The release of the traction, however, is very smooth. This form of φ was employed for the numerical analysis in the present investigation.

3.2. Simulation of tube splitting with the conical die

Only the test set-up using the non-symmetrical conical die was modelled. A half-tube was modelled using appropriate symmetry conditions. The finite element mesh is shown in Fig. 8. A cylindrical coordinate system is employed to locate the tube and die position. Axis x is in the axial direction of the tube and θ is measured from the symmetry plane. The smallest elements in the mesh were 0.3125 mm × 0.3125 mm, these being along the crack propagation line along which interface elements were generated.

The cone was 20 mm long and had a circular nose of radius 24.3 mm. The nose of the cone was initially placed at $x = 0$, the end of the tube with an initial 15 mm long crack. The base was non-symmetric with the following varying radius

$$r = 30.8 \text{ mm} \quad \text{for } \theta \leqslant 45^\circ, \tag{14}$$

$$r = 24.3 + (30.8 - 24.3)\sin^4\left(\frac{180 - \theta}{135} \times 90\right) \text{ mm} \quad \text{for } 45^\circ < \theta < 180^\circ. \tag{15}$$

The maximum cone angle is 18°, the same as that of unsymmetrical cone die used in the tests. The die was only allowed to move in the axial direction to split the tube which is fixed at the far end $x = 300$ mm.

The predictions (with and without friction) and experimental load–displacement curves for the non-symmetric conical die tests are shown in Fig. 9. There is a big scatter in the experimental curves for different tubes due to the lubrication of the die and tube, some being well lubricated and some probably not so. Friction was considered in the FE model using a friction coefficient of 0.3 (Bowden and Tabor, 1964). This prediction is well within the experimental range. A frictionless FE model gives a much lower load/displacement curve. The prediction shows that the crack starts to propagate when the die had moved a distance of 11 mm, common to both experiments and models. However, the crack growth rate is slower than the movement of the die in the early stage. The crack tip begins to catch up with the die movement when the base of the conical die has also entered into the tube. The steady state is gradually reached after the conical die has been pushed around 40 mm into tube. The moving crack tip remains about 3 mm ahead of the nose of the cone. These crack propagation features echo the variations in the load/displacement curve at different stages.

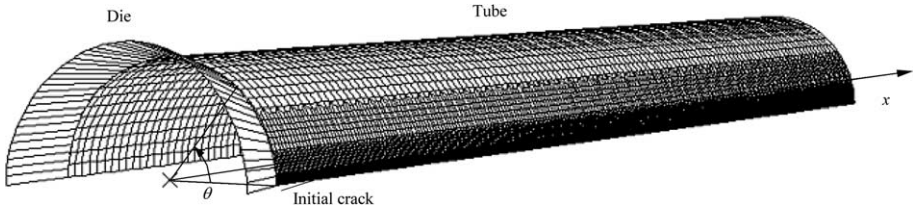

Fig. 8. Finite element mesh of the half model of the tube and die and the coordinate system.

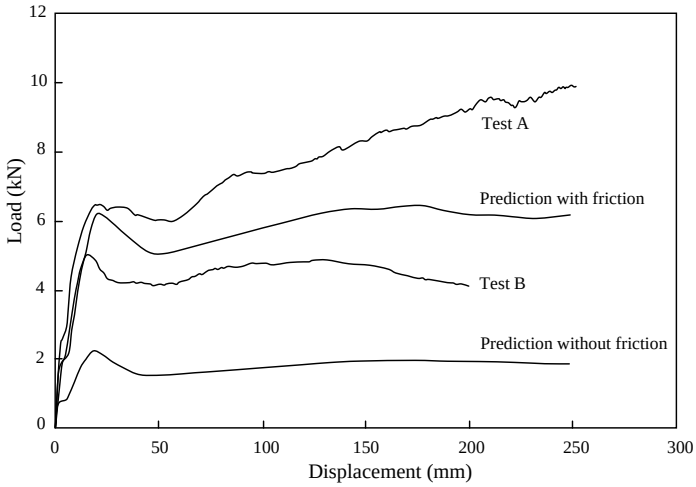

Fig. 9. Load versus displacement curves of the cone die.

Including friction or not in the FE model does not make significant difference to either the phenomena involved in the deformation of the tube or the stress and strain field in the split tube. Fig. 10 gives the predicted tube deformation after the split has occurred. It can be seen that the cracked end was almost flattened and two ripples are clearly predicted on the flaps of the tube in the middle, matching the experimental observation very well. The above comparison between the prediction and experimental results indicates that the major features of the test are well simulated by the FE model. The stress and stress fields in the tube are therefore likely to be reliable.

The history of the axial membrane strain at the cross-section in the middle of the tube length ($x = 150$ mm) is shown in Fig. 11. $\theta = 0$ indicates the fracture edge. The axial strain experiences a significant variation when the die approaches and passes the cross-section. After the cone base has passed the cross-section and moves further forward, its direct effect in changing the strain at the cross-section stops and constant strain states are established. Due to the removal of the external load, the deformation reaches

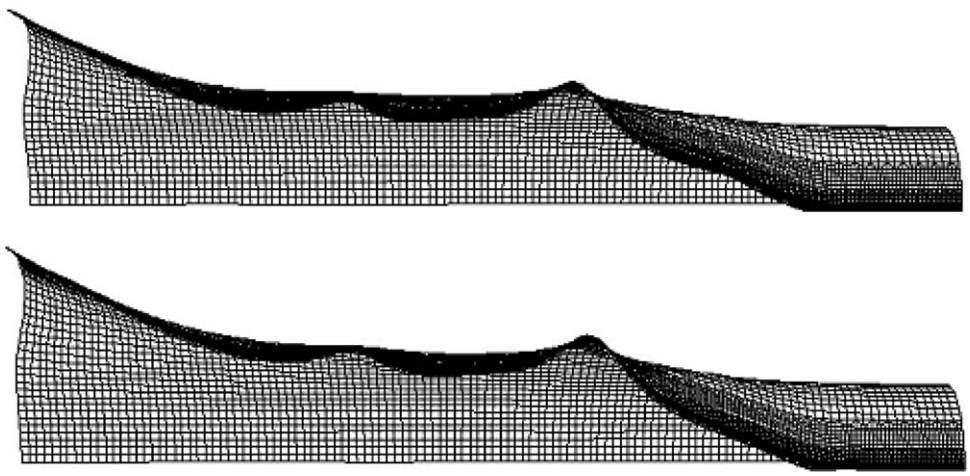

Fig. 10. Predicted deformation of the tube split by unsymmetrical cone die (with and without friction).

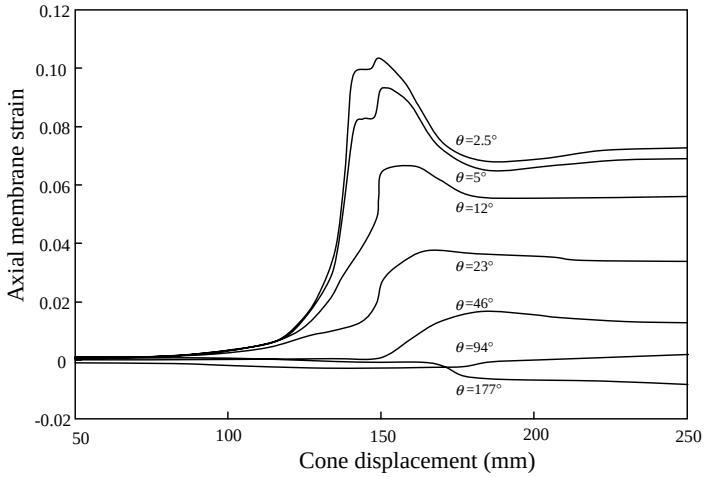

Fig. 11. History of the axial membrane strain at tube cross-section $x = 150$ mm as cone moves forward.

a steady state and there is only slight variation in strain caused by redistribution. It can be seen that there are three zones in the circumferential direction in which axial stretching of the tube varies.

The first zone extends from the fracture edge to around 10 mm ($0° < \theta < 23°$) from it. Material in this region is stretched in the axial direction when the crack tip approaches the cross-section (cone displacement = 130 mm) and reaches its peak when fracture takes place at the cross-section (cone displacement = 150 mm). The values of the axial strain experienced in this zone exceed 0.04, well into the plastic range. Elastic recovery of the axial strain occurs as the contact with the conical die goes past the cross-section. After the cone base has passed the cross-section, the axial strain reduces by about 0.02 on average.

The neighbouring zone is also approximately 10 mm wide ($23° < \theta < 46°$). Material in this zone has a large increase of axial strain when the cone die is pushed through the cross-section. The reduction of the axial strain in this region is much less noticeable compared with those in the first region after the gradual movement away of the die. The third zone contains the part of the cross-section far away from the edge, much wider than the first two zones. Little axial stretching and slight contraction happens in this zone.

The history of the circumferential membrane strains is shown in Fig. 12. The material at the fracture edge contracts first when the cone die approaches due to the Poisson's effect of the axial stretching and meridional re-bending. The meridional re-bending phenomenon ahead of the crack tip can be seen clearly in Figs. 3 and 4. Significant stretching in the circumferential direction only happens when the crack front is very close to the cross-section primarily as a result of the radial expansion by the die and this is confined to a very narrow region (less than 2 mm wide, $\theta < 5°$) near the fracture edge. Further stretching in the circumferential taking place over the entire section is mainly caused by the cone base. Overall, the circumferential strain in the tube is much lower than the axial strain, confirming the assumption made by Abbassian and Calladine (1989) that the axial stretching was the prime mode of deformation of the pipe wall.

Fig. 13 shows the distribution of the axial and circumferential strain at the mid cross-section of the tube for cone displacements of 150 mm and 200 mm. The circumferential strain is much higher than the axial component in the region very close to the fracture edge. This shows that fracture is caused primarily by radial expansion. The very high magnitude of the circumferential strain at the fracture edge indicates the presence of the singular behaviour at the crack tip.

Fig. 14 gives the distribution of the generalised axial stress (i.e. stress resultant over the tube thickness) along the tube generator after the cone die moved 200 mm inside the tube. It can be seen that there is a band, 10 mm wide and 100 mm long, just behind the crack tip and close to the fracture edge, where

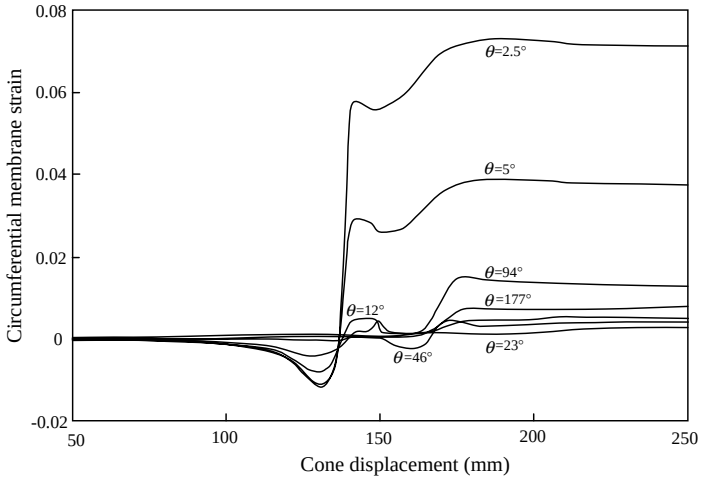

Fig. 12. History of the circumferential membrane strain at tube cross-section $x = 150$ mm as cone moves forward.

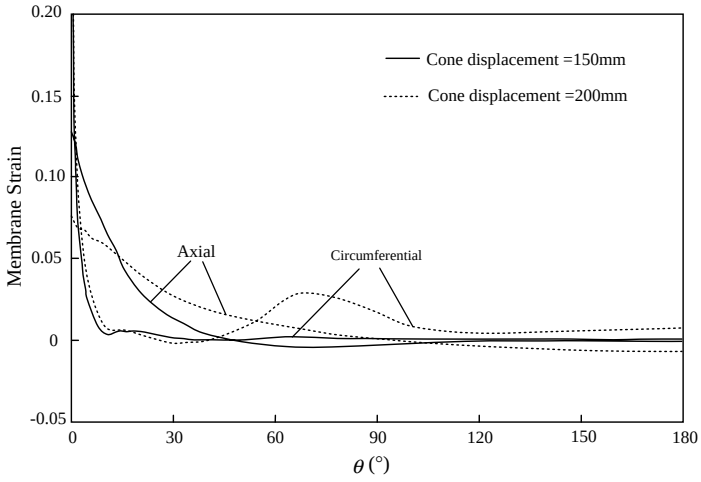

Fig. 13. Distribution of axial and circumferential membrane strains around tube cross-section $x = 150$ mm.

compressive generalised stress exists in the axial direction. High tensile stress is found ahead of the crack tip and close to the fracture edge, stretching the material in the axial direction. The distribution of generalised axial stress around the mid cross-section of the tube is shown in Fig. 15. As the cone passes the cross-section, compression zone at the fracture edge widens and reaches a steady width of 10 mm. Tensile and compressive axial stress also presents in the other parts of the cross-section to give a resulting zero force for the entire section.

In the above tube split problem, the crack tip travels about 3 mm ahead of the nose of the moving cone. The cone die applied a distributed transverse load to tube wall behind the crack tip, simulating the residual pressure acting on the fracture flaps behind the crack tip by the venting of high-pressure gas.

To investigate the effect of the internal pressure acting ahead of the fracture, tube splitting by a die with smaller cone angle was also modelled. The varying radius of the base of the die was as follows

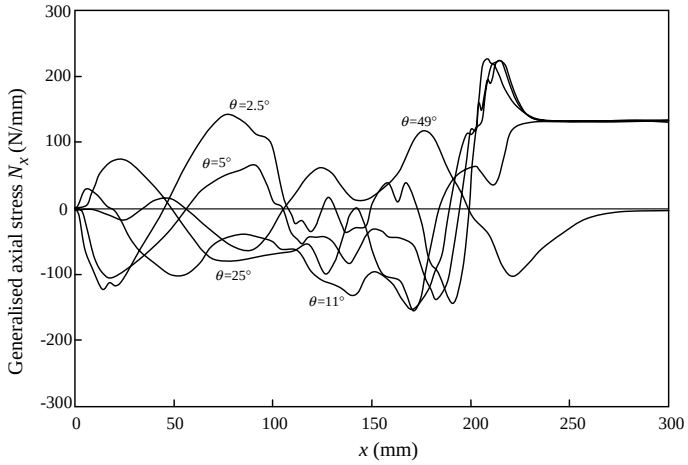

Fig. 14. Distribution of generalised axial stress N_x along the tube generator direction (cone displacement = 200 mm).

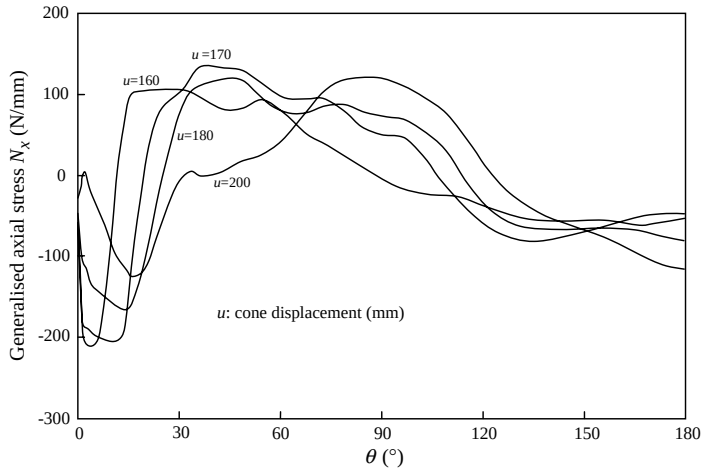

Fig. 15. Distribution of generalised axial stress N_x around tube cross-section $x = 150$ mm.

$$r = 27.83 \quad \text{for } \theta \leqslant 45^\circ, \tag{16}$$

$$r = 24.3 + (27.83 - 24.3)\sin^4\left(\frac{180 - \theta}{135} \times 90\right) \quad \text{for } 45^\circ < \theta < 180^\circ. \tag{17}$$

This corresponds to a 10° maximum cone angle. The cone is still 20 mm long.

The numerical analysis shows that the crack tip was kept around 16 mm behind the nose of the travelling cone. The conical die applied extensive transverse load to the tube wall ahead of the crack tip, i.e. the driving force for the crack propagation is from the internal pressure. The deformed tube split by this small conical die is shown in Fig. 16. No ripples are evident on the flaps of the tube.

The histories of the axial and circumferential membrane strains at the mid cross-section of the tube ($x = 150$ mm) are shown in Figs. 17 and 18. For this small cone angle, circumferential stretching is the

Fig. 16. Predicted deformation of the tube split by a cone with cone angle = 10°.

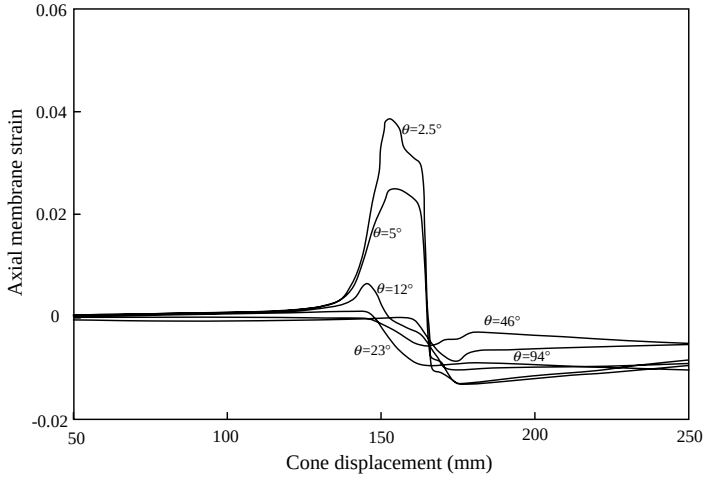

Fig. 17. History of the axial strain at cross-section $x = 150$ mm of the tube split by a small angle cone die.

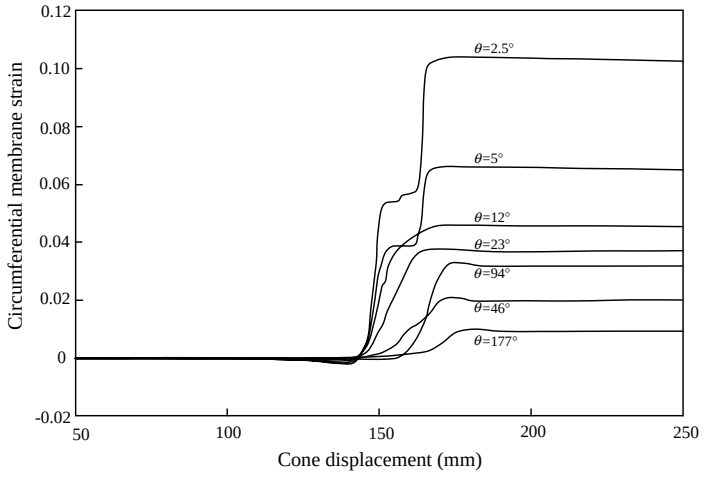

Fig. 18. History of the circumferential strain at cross-section $x = 150$ mm of the tube split by a small angle cone die.

prime mode of deformation of the tube wall. The entire cross-section was stretched in the circumferential direction when the cone passes it. Axial stretching only occurs very close to the fracture edge when the cone approaches. Once the die reaches the cross-section, the tube starts to contract in the axial direction due to

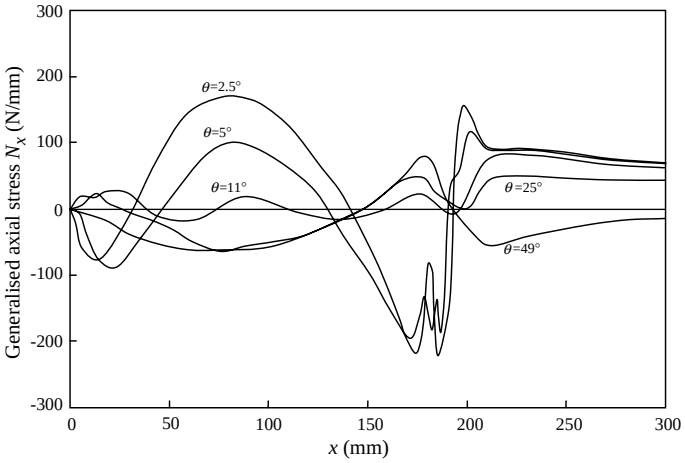

Fig. 19. Distribution of generalised axial stress N_x at cross-section $x = 150$ mm of the tube split by a small angle cone (cone displacement = 200).

the circumferential stretching and the plastic incompressibility. Such a deformation cannot generate residual axial compressive stress sufficient to produce local buckling. Fig. 19 gives the distribution of the generalised axial stress along the tube generator after the cone die moved 200 mm inside the tube. It can be seen that a compressive generalised stress does exist in the axial direction. However, the compression zone along the fracture edge zone is very narrow and short.

3.3. Simulation of tube tearing with wedge die

A half-tube model was also adopted to simulate the tearing test on a 200 mm long tube with a 15 mm long initial crack. The basic meshing of the tube was analogous to that used for the conical die test regarding the number and distribution of elements and element sizes in the vicinity of the potential fractures. However in the wedge die test, there are three traction components acting in the crack extension plane. Numerical results show that it is a Mode III dominated mixed mode crack problem. The three modes are approximately in the following proportions

$$G_{\mathrm{I}} : G_{\mathrm{II}} : G_{\mathrm{III}} = 10 : 16 : 74. \tag{18}$$

The wedge was put in contact with the tube from the beginning. No crack propagation occurred at first and the strip between the two initial cracks begun to curl. As the wedge reached the initial crack tip, the crack began to propagate, and the crack tip was very close to the wedge surface afterwards. Fig. 20

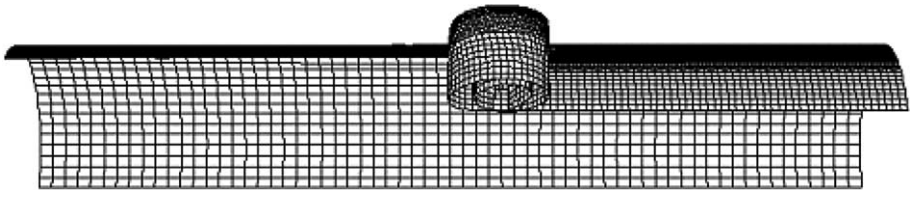

Fig. 20. Prediction of the deformed tube torn at a wedge displacement level of 100 mm.

shows the deformed tube. There is a curling strip and the fracture edge on the tube stays straight. The prediction shows the characteristics of the deformation and compares well with the experimental observations.

The distributions of the membrane strains in the remaining part of the fractured tube, not the strip, are given in Figs. 21 and 22 at a wedge die displacements of 102 mm. It can be seen that the magnitude of these strains are much lower than those in the cone die tests. As the wedge moves, there is only a very small change in the axial membrane strain behind the crack tip, except in the region near the fracture edge (less than 2 mm wide, $38° < \theta < 43°$). As a result, large compressive stress in the axial direction cannot be expected, as confirmed in Fig. 23. No local buckling would occur along the fracture edges.

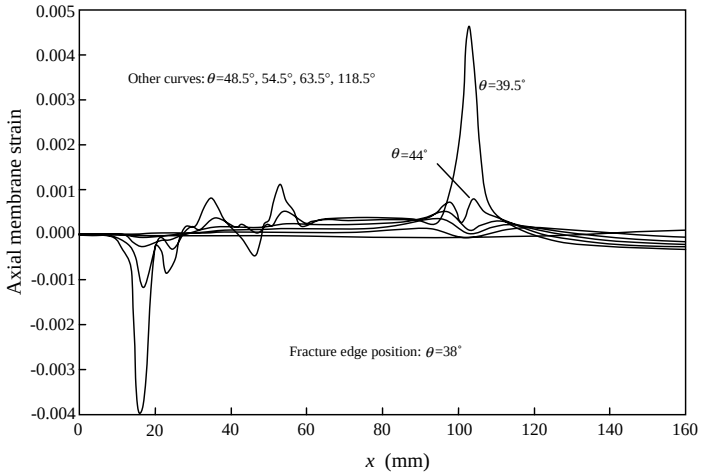

Fig. 21. Distribution of axial membrane strain along the tube generator direction (wedge displacement = 100 mm).

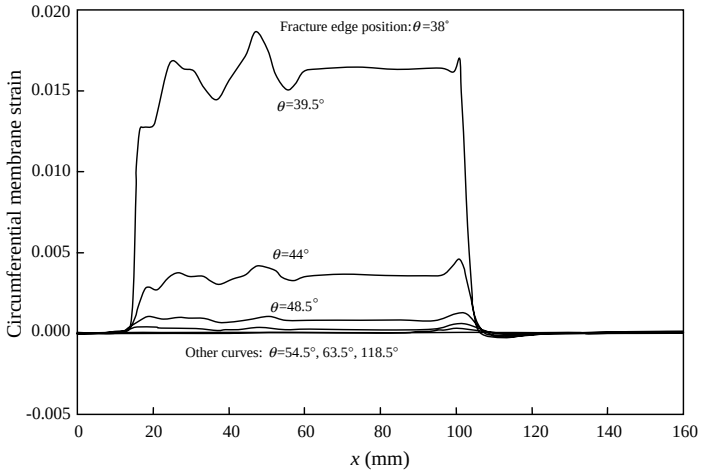

Fig. 22. Distribution of circumferential strain along the tube generator direction (wedge displacement = 100 mm).

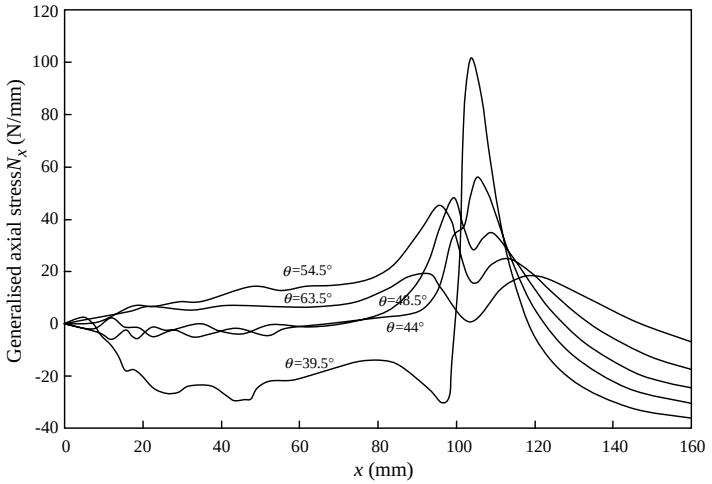

Fig. 23. Distribution of generalised axial stress N_x along the tube generator direction (wedge displacement = 100 mm).

4. Summary of mechanism producing wavy fracture edges

The wavy edge is a local buckling phenomenon in the plastic wake (boundary layer) caused by the residual compressive stress in the direction parallel to the crack. It can only happen under the following conditions:

(a) Plastic strain in the direction parallel to the fracture edge has to exist and has varying magnitude along the direction perpendicular to the fracture edge, extensional close to the edge and elastic or compressive plastic in the other parts of the cross-section of the thin-walled tube.
(b) The magnitude of the extensional plastic strain is large enough to produce sufficient residual compressive stress after unloading.
(c) The extensional plastic zone close to the fracture edge is wide enough.

It is well known that there is a plastic zone around the crack tips in ductile metal structures. Generally the plastic zones are very small and the largest plastic strain component is in the direction perpendicular to the crack. The strain parallel to the crack is often compressive due to the plastic incompressibility.

Among the tests conducted in the present investigation, only the conical die with relatively large cone angle generated a wide plastic zone with significant axial stretching parallel to the fracture edge and produced the wavy fracture edge. The conical die with small cone angle and wedge die cannot provide the conditions required for the occurrence of local buckling along the fracture edge.

As the experiment and numerical analysis shows, during the progressive fracture process, the moving conical die with relatively large cone angle is always behind the propagating crack tip. This means the conical die applies an outward transverse load to the two flaps of the fracturing tube behind the crack tip. However, the wedge provides a load to the tearing strip. The small-angle conical die generates a transverse load which acts on the tube ahead of the crack tip instead of the flaps behind the crack front. The position and direction of the load applied to the tube plays a key role in producing the wavy fracture edge. A transverse load acting on the tube wall behind the crack tip is a necessary condition.

After crack propagation, the stiffness of the tube is reduced dramatically in the cracked region in the circumferential direction. A transverse load acting on the cracked part of the tube can expand the tube in the radial direction to a large extent. The circular shape of the cross-section of the tube is flattened,

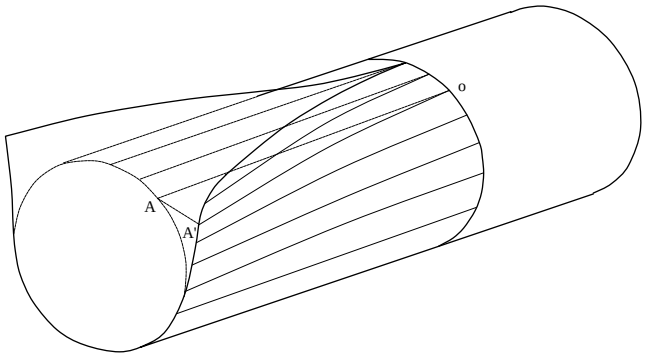

Fig. 24. Deformation of the tube around the crack tip.

especially near the crack surfaces. Fig. 24 shows the deformation of the tube around the crack front. Consider two points A and O originally located on the same generator of the tube which is a small distance away from the crack line. After the crack propagates to the cross-section where point O is located, a transverse load, exerted onto the tube wall by the conical die, pushes the two flaps behind the crack tip away from each other. During this process, the cross-section can hardly move in the axial direction due to the constraint from the other part of the tube. However, point A moves a big distance to a new position A' in the tube cross-section plane and point O nearly remains at its original position. Obviously, OA is a straight line and OA' is a curve. A surface of double curvature having a non-zero Gaussian curvature is generated. This requires that severe axial stretching has to take place in the vicinity of the crack tip during the expansion process of the tube. The nearer the material is to the crack surface, the severer is the axial stretching. A wide non-uniform plastic zone is thus formed behind the crack tip.

As the conical die moves forward and the crack propagates, there is no transverse load acting on the fractured flaps left behind. Further expansion of the fractured flaps of the tube cannot be expected due to the constraint from the neighbouring parts and the deformation reaches a steady state, two parallel fractured edges. Under the constraint of the remaining part of the tube that has not undergone plastic deformation, sufficient axial residual compressive stress can be produced in the plastic wake adjacent to the edges leading to local buckling and the wavy fracture edges.

5. Assessment of wavy fracture edge on the wreckage of fuselage skin

The mechanism discussed above can explain how the ripple was formed on the wreckage of fuselage skin. Transverse load acting on the fuselage skin is a necessary condition for wavy-edged fractures. This load could come from an internal explosion, instead of external agencies such as wind loads. If an internal explosion occurs inside a fuselage, there will be high pressures acting on the skin. Once a crack initiates in the skin, the high-pressurised gas escaping behind the crack tip drives crack propagation. This escaping gas also expands the fractured skin in the radial direction and stretches the material axially in a qualitatively similar manner to the mechanism in the quasi-static conical die tests. As the crack propagates, an extensive stretched plastic wake is left behind.

The local buckling along the fracture edge in the present problem can be treated approximately as a plate with three simply supported edges and one free edge under compression. Solutions for the elastic buckling of a thin plate can be found in textbook. The critical buckling strain is given as (Timoshenko and Gere, 1963)

$$\varepsilon_{cr} = \left(0.456 + \frac{b^2}{a^2}\right)\frac{\pi^2 t^2}{12b^2}, \tag{19}$$

where a and b are the length and width of the plate, t the thickness.

For the tested aluminium tube of a 50.8 mm diameter, the dimension of the compression zone along the fracture edge has been found to be 100 mm × 10 mm. A fuselage has a big diameter, normally greater than 3 m. The plastic zone under stretching will be much larger than that in the tubes tested. Suppose $a = 1000$ mm, $b = 100$ mm, and $t = 5$ mm for a fuselage skin wreckage, then the critical buckling strain is

$$\varepsilon_{cr} = 0.466 \times \frac{\pi^2 \times 5^2}{12 \times 100^2} \approx 0.001\ (0.1\%). \tag{20}$$

This strain level is very low, not exceeding the yield strain, and can be achieved easily by the strain relaxation after crack propagation as shown by the tube test which produced a 0.02 reduction in the axial strain. That is the reason why wavy edges on fracture edges generated by internal overpressure are likely to be observed on the wreckage of fuselage skin after explosion.

6. Conclusions

Ripples have sometimes been observed on the edges of certain fuselage skin pieces recovered from the wreckage of aeroplanes destroyed by explosives. A preliminary set of quasi-static experiments has been performed and finite element modelling has been carried out on aluminium tubes to investigate the conditions leading to this phenomenon.

The experimental and numerical results have shown that extensive tensile axial plastic strain has to exist along the fracture edge to cause residual compressive stress in the direction parallel to the edge. Buckling can then take place on the flaps to form the wavy edge.

It has been found that the phenomenon can be produced by applying a localised, radially outward transverse load behind the crack tip that drives the crack. This load expands the potential flaps in the radial direction, stretching the material in the hoop direction and, crucially, in the direction parallel to the crack to a great extent. Both the magnitude of the tensile plastic strain and the size of the stretching zone are large compared with the other alternative Mode III tearing of the tube. Other loading conditions, e.g. internal pressure acting on the tube wall ahead of the crack tip, can fracture the tube as well, but are unlikely to produce such phenomenon.

This brief investigation confirms the result from studies of similar phenomena described in the literature and strongly supports the contention that the wavy edge on the wreckage of the fuselage skin has to be caused by some kind of transverse load acting on it, most likely that produced by an internal explosion.

Acknowledgments

We are grateful to Professor C.R. Calladine, FRS, FREng for comments on an earlier version of this paper. We would like to record our thanks to the Office of the Attorney General of British Columbia, Canada for financial support for this work.

References

Abbassian, F., Calladine, C.R., 1989. On the deformation of the pipe wall during propagation of a ductile crack in a high-pressure gas pipeline. Journal of pressure Vessel Technology 111, 47–57.

Atkins, A.G., 1987. On the number of cracks in the axial splitting ductile metal tubes. International Journal of Mechanical Science 29, 115–121.

Bowden, F.P., Tabor, D., 1964. The Friction and Lubrication of Solids. Oxford University Press, London.

Freund, L.B., Parks, D.M., Rice, J.R., 1976. Running ductile fracture in a pressurised line pipe. In: Mechanics of Crack GrowthASTM STP 590. American Society for Testing and Materials, pp. 243–262.

HKS, 2001. ABAQUS/Standard User's Manual, Version 6.2.

Ives, K.D., Shoemaker, A.K., McCartney, R.F., 1974. Pipe deformation during a running shear fracture in line pipe. ASME Journal of Engineering Materials and Technology 96, 309–317.

Needleman, A., 1987. A continuum model for void nucleation by inclusion debonding. Journal of Applied Mechanics 54, 525–531.

Reddy, T.Y., Reid, S.R., 1986. Axial splitting of circular metal tubes. International Journal of Mechanical Science 28, 111–131.

Shannon, R.W.E., Wells, A.A., 1974. A study of ductile crack propagation in gas pressurised pipelines. In: Proceedings of the International Symposium on Crack Propagation in Pipelines. The Institution of Gas Engineers, Newcastle Upon Tyne, England, Paper 17.

Steverding, B., Nieberlein, V., 1974. Fracture of pressurized cylindrical shells. Engineering Fracture Mechanics 6, 387–395.

Timoshenko, S.P., Gere, J.M., 1963. Theory of Elastic Stability, second ed. McGraw-Hill Book Company.

Tvergaard, V., Hutchinson, J.W., 1992. The relation between crack growth resistance and fracture process parameters in elastic–plastic solids. Journal of the Mechanics and Physics of Solids 40, 1377–1397.

Xu, X.P., Needleman, A., 1994. Numerical simulation of fast crack growth in brittle solids. Journal of the Mechanics and Physics of Solids 42, 1397–1434.

Zou, Z., Reid, S.R., Li, S., 2003. A continuum damage model for delaminations in laminated composites. Journal of the Mechanics and Physics of Solids 51, 333–356.

Zou, Z., Fok, S.L., Oyadiji, S.O., Marsden, B.J., 2004. Failure predictions for nuclear graphite using a continuum damage mechanics model. Journal of Nuclear Materials 324, 116–124.